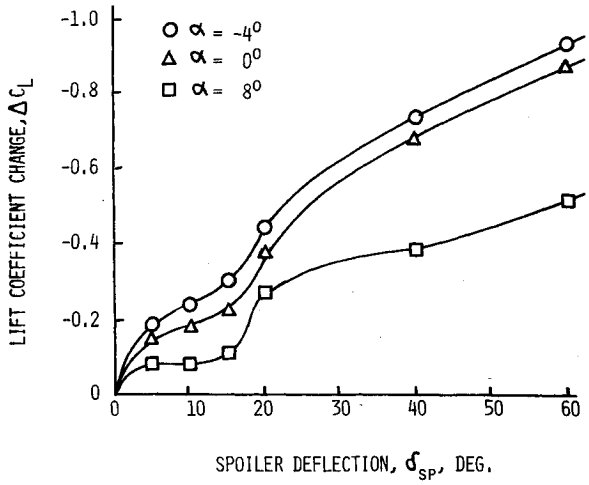

Fig. 4 Spoiler effectiveness, flap deflection 30 deg, 15% chord spoiler, 85% chord hingeline.

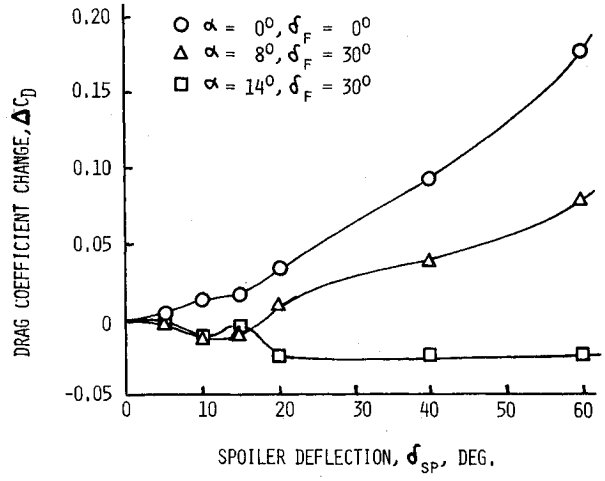

Fig. 5 Spoiler drag performance, 15% chord spoiler, 85% chord hingeline.

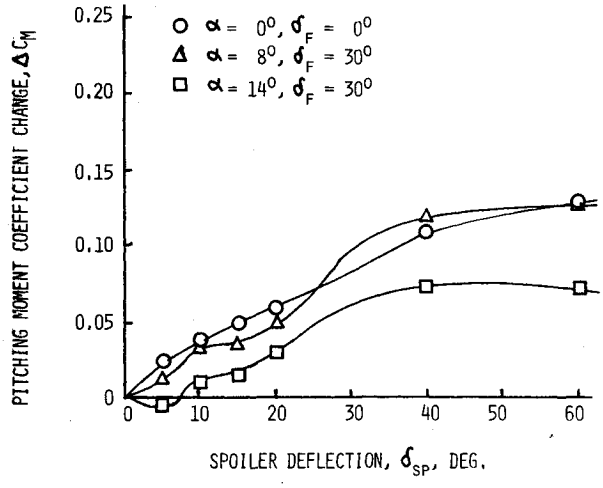

Fig. 6 Spoiler pitching moment performance, 15% chord spoiler, 85% chord hingeline.

landing configuration is best represented by the two curves for flap deflection of 30 deg and wing angles of attack of 8 and 14 deg. Spoiler deflection has little effect on drag with the wing operating at these high angles of attack, due primarily to the substantial boundary-layer thickening at high angles of attack. The drag reduction for large spoiler deflection angles at a wing angle of attack of 14 deg is about 10% of the profile drag of the wing with flap nested.

The effect of spoiler deflection on pitching moment performance as shown in Fig. 6 suggests an aid to the pilot in the approach-to-landing configuration. The nose pitch-down tendency due to flap deployment is reduced (positive ΔC_m) as the spoilers are deflected for flight path control.

Wind-tunnel tests have demonstrated the capability of the GA(W)-1 airfoil equipped with plain-type spoilers to produce effective flight path control in the approach to landing configuration. The 15% chord spoiler with hingeline location at the 85% chord position offers the best performance by producing large (negative) lift increments and small changes in drag and pitching moment performance.

References

[1] Weick, F. and Wenzinger, C., "Preliminary Investigation of Rolling Moments Obtained with Spoilers on Both Slotted and Plain Wings," NACA TN 415, 1932.

[2] Roskam, J., Kohlman, D. L., and Wentz, W. H., "Spoilers for Roll Control of Light Airplanes," AIAA Paper 74-861, Anaheim, Calif., Aug. 1974.

[3] Kohlman, D. L., "Flight Test Results for an Advanced Technology Light Airplane Wing," SAE Business Aircraft Meeting, Wichita, Kan., SAE Paper 740368, April 1974.

[4] Wentz, W. H. Jr., "Reflection-Plane Tests of Spoilers on an Advanced Technology Wing," SAE Business Aircraft Meeting, Wichita, Kan., SAE Paper No. 760482, April 1976.

[5] Neuhart, D. H., "An Experimental Investigation of the Potential Performance of Plain-Type Spoilers Applied to the GA(W)-1 Wing," M.S. Thesis, Dept. of Aerospace Engineering, University of Missouri – Rolla, Rolla, Mo., Jan. 1977.

[6] Rice, R. K. and Oetting, R. B., "Preliminary Wind Tunnel Tests of a Finite Aspect Ratio High Performance General Aviation Wing," *Journal of Aircraft*, Vol. 13, March 1976, pp. 223-224.

Calculation of Vortex Breakdown Locations for Flow over Delta Wings

James D. Wilson*
Air Force Flight Dynamics Laboratory, Wright-Patterson AFB, Ohio

Nomenclature

c,C	= circulation parameter, rw; value at $r=R$
l	= midchord of delta wing
R	= vortex core radius
u,v,w	= axial, radial, and swirl velocity components
U,W	= axial and swirl velocity components at $r=R$
x,r	= axial and radial coordinate directions
α	= angle of attack
Λ	= angle of sweep of wing leading edge
ϕ	= $\cos^{-1}(\cos\alpha \sin\Lambda)$

Introduction

THE relationship between the breakdown of high-swirl vortex cores observed in experiments and a corresponding failure of the quasicylindrical approximation of the Navier-Stokes equations has been reported by several investigators. Hall[1] used a finite-difference scheme to solve the quasicylindrical equations with initial and outer boundary conditions supplied by the experimental results of Kirkpatrick[2] for swirling flow in a duct. Hall found that con-

Received May 26, 1977.
Index categories: Aerodynamics; Subsonic Flow.
*Captain USAF, Aerodynamic Analyst. Member AIAA.

verged solutions to the equations could not be obtained near the experimentally determined breakdown location of the core (the difference in location was within two diameters of the viscous core). The failure of the quasicylindrical approximation is associated with the rapid retardation of the axial flow producing large axial gradients in the vicinity of core breakdown.

Hall also performed computations in which the initial amount of swirl and the outer pressure field encountered by the vortex core were varied. The results indicated that the axial location at which the equations failed varied in the same way as the experimentally observed breakdown location varied. Working with the integral form of the equations, Bossel[3] and Raat[4] have also shown the effects of swirl and external pressure gradient on breakdown location.

Based on the demonstrated ability of the quasicylindrical equations to model observed vortex core behavior, the equations are used to predict the breakdown location for the strong vortex that forms when leading-edge separation occurs on highly swept delta wings. The basic assumption of the flow model is that the viscous, rotational vortex core is confined to a narrow region and has a negligible effect on the shape and location of the spiral vortex sheet which springs from the wing leading edge. Consequently, a potential flow method capable of modeling the vortex sheet roll-up is used to supply the outer boundary conditions for the vortex core. The core model also requires initial boundary conditions on the velocity profiles (or swirl parameter in this formulation) which are unknown in advance. By obtaining solutions to the core model for a range of initial conditions, a correlation is obtained for the initial value of the swirl parameter that results in the calculations matching experiment for vortex breakdown location.

Flow Model

The vortex core model is essentially the one developed by Raat.[4] It has been modified to include axial variation of circulation to simulate vorticity being fed into the core from the rolling up vortex sheet. The governing equations are the quasicylindrical form of the incompressible Navier-Stokes equations (see Refs. 1, and 3-5). Following the approach of Ref. 4, the equations are put into integral form.

$$\frac{\mathrm{d}}{\mathrm{d}x}(U^2\Theta)+U\frac{dU}{dx}\Delta^*=-\pi\int_0^R\frac{\partial c^2}{\partial x}\frac{\mathrm{d}r}{r} \tag{1}$$

$$\frac{\mathrm{d}}{\mathrm{d}x}(UC\Psi)-2\pi\frac{dc}{dx}\int_0^R ur\mathrm{d}r=4\pi\nu C \tag{2}$$

where

$$\Theta=\int_0^R\left(1-\frac{u}{U}\right)\frac{u}{U}2\pi r\mathrm{d}r$$

$$\Delta^*=\int_0^R\left(1-\frac{u}{U}\right)2\pi r\mathrm{d}r$$

Table 1 Experimental vortex breakdown locations for flow over delta wings

			Breakdown location, x/l			
AR	Λ, deg	α, deg	Ref. 9	Ref. 10	Ref. 11	Ref. 12
1.46	70	30		0.70	0.77	>1.0
1.46	70	35		0.38	0.38	0.42
1.46	70	40		0.20	0.17	0.22
1.86	65	20	0.75	>1.0		
1.86	65	25	0.38	0.50		
1.86	65	30	0.23	0.32		
1.86	65	35		0.20		
2.31	60	15	0.75	0.80		
2.31	60	20	0.40	0.50		
2.31	60	25	0.24	0.23		

$$\Psi=\int_0^R\left(1-\frac{c}{C}\right)\frac{u}{U}2\pi r\mathrm{d}r$$

The axial velocity and circulation profiles from Ref. (4),

$$u/U=1+[(r/R)^2-1]^3[(3-3u_0-u_2)(r/R)^2+(1-u_0)] \tag{3}$$

$$c/C=1+[(r/R)^2-1]^3 \tag{4}$$

are substituted in Eqs. (1) and (2) to give the following set of equations.

$$\lambda^2Pf_1+\frac{73}{120}k-\frac{1}{2}k\,\ell nP+\int_0^X\left(\ell nP\frac{\mathrm{d}k}{\mathrm{d}X}+\lambda Pf_2\frac{\mathrm{d}\lambda}{\mathrm{d}X}\right)\mathrm{d}X=A_1 \tag{5}$$

$$\lambda Pf_3+\int_0^X\frac{\lambda}{10}P(5f_3-f_4)\frac{\mathrm{d}\ell nk}{\mathrm{d}X}\mathrm{d}X-4X=A_2 \tag{6}$$

$$\lambda^2(u_0-1)-\frac{37}{10}\frac{k}{P}-\int_0^X\frac{8\lambda u_2}{P}\mathrm{d}X=A_3 \tag{7}$$

where

$$\lambda=U(X)/U(0) \qquad k=[C(X)/R(0)U(0)]^2$$

$$P=[R(X)/R(0)]^2 \qquad X=\nu x/U(0)R^2(0)$$

$$f_1=\frac{1}{7}\cdot\left(\frac{4}{5}+\frac{6}{5}u_0+\frac{1}{15}u_2-2u_0^2-\frac{1}{36}u_2^2-\frac{5}{12}u_0u_2\right)$$

$$f_2=\frac{2}{5}\cdot\left(1-u_0-\frac{1}{8}u_2\right)$$

$$f_3=\frac{1}{36}\cdot\left(3+11u_0+u_2\right)$$

$$f_4=3+2u_0+\frac{1}{4}u_2$$

Equation (7), which is derived from Eq. (1) evaluated at $r=0$, is required to provide three equations to solve for the unknowns $u_0(X)$, $u_2(X)$, and $P(X)$. The constants of integration A_1, A_2, and A_3 are evaluated from specification of $u_0(0)$, $u_2(0)$, and $k(0)$. Both λ and k are functions of X giving the variation in axial velocity and circulation, respectively, at the outer edge of the core.

One of the key parameters in describing vortex flows is the ratio of the swirl to the axial component of velocity. Following Ref. (3) a swirl parameter is defined based on conditions in the core.

$$S=\frac{(\mathrm{d}w/\mathrm{d}r)_{r=0}\ \ (r)\text{ at }w_{\max}}{u_0U}=\frac{1.994}{\lambda u_0}\sqrt{\frac{k}{P}} \tag{8}$$

The outer conditions for the vortex core λ and k are supplied by a subsonic potential flow-panel method that can calculate the flowfield for a wing experiencing leading-edge separation. The method was formulated and a computer code developed by Weber et al.,[6] Johnson et at.,[7] and Brune et al.[8] The shear layer separating from the wing leading edge is represented by a free doublet sheet while the vortex core is represented by a line vortex connected to the free sheet by a kinematic feeding sheet. Values for λ and k are obtained, respectively, from the jump in velocity potential and the average axial velocity along the column of panels comprising the edge of the free sheet that is connected to the feeding sheet.

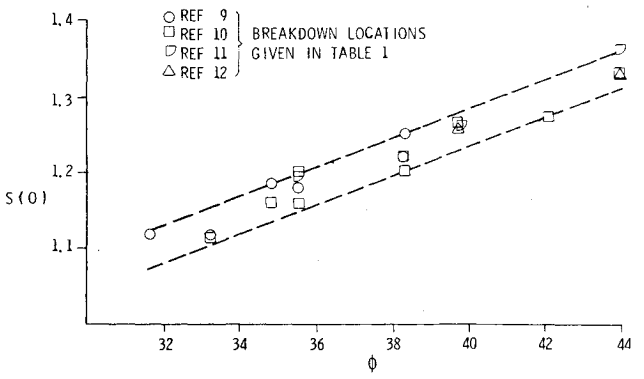

Fig. 1 Correlation for initial value of the swirl parameter for calculating experimentally observed vortex breakdown locations.

Calculation of Breakdown Locations

The experimental data from Refs. 9-12 for vortex breakdown location for flow over thin delta wings in low, subsonic flow is given in Table 1. The spread in the experimental data is usually attributed to slight differences in geometry, particularly at the leading edge (see for example Ref. 13). As indicated in Ref. 1, changes due to Reynolds number variations in these experiments probably do not exceed 10-15%.

It was attempted to match the experimental data using the vortex core model. To provide the edge boundary conditions, the potential flow program was run for the three delta wings at the same angles of attack as listed in Table 1. For all runs, the wing was represented by 25 panels and the free sheet by 40 panels with 5 evenly spaced panels being in the chordwise direction.

As previously indicated, the initial values of the parameters in the axial velocity profile u_0 and u_2 must be specified. For the series of calculations made $u_2(0)=0$ and $u_0(0)$ was varied [$S(0)$ was varied, see Eq. (8)]. It was found that the experimental vortex breakdown locations could be matched by choosing a particular value of $u_0(0)$.

The results are shown in Fig. 1 as a plot of the initial value of the swirl parameter $S(0)$ and the angle ϕ between the wing leading edge and the freestream direction. Each point in the figure represents the initial condition of swirl that results in core breakdown at the same x/l location as an experimental point in Table 1. For the fairly scattered experimental data matched, the points in the figure collapse to a band approximately 0.05 wide in $S(0)$. The correlation of Fig. 1 provides the initial condition required to compute vortex breakdown for delta wings using the quasicylindrical flow model.

References

[1] Hall, M. G., "Vortex Breakdown," *Annual Review of Fluid Mechanics*, Vol. 4, 1972, pp. 195-218.

[2] Kirkpatrick, D.L.I., "Experimental Investigation of the Breakdown of a Vortex in a Tube," RAE Tech. Note No. Aero. 2963, 1965.

[3] Bossel, H. H., "Vortex Equations: Singularities, Numerical Solution, and Axisymmetric Vortex Breakdown," NASA CR-2090, July 1972.

[4] Raat, J., "Vortex Development and Breakdown," AFFDL-TR-75-69, May 1975.

[5] Hall, M. G., "A Numerical Method for Solving the Equations for a Vortex Core," Royal Aircraft Establishment, RAE Tech. Rept. No. 65106, May 1965.

[6] Weber, J. A., Brune, G. W., Johnson, F. T., Lu, P., and Rubbert, P. E., "A Three-Dimensional Solution of Flows over Wings with Leading-Edge Vortex Separation," AIAA Paper 75-866, Hartford, Conn., June 1975.

[7] Johnson, F. T., Lu, P., Brune, G. W., Weber, J. A., and Rubbert, P. E., "An Improved Method for the Prediction of Completely Three-Dimensional Aerodynamic Load Distributions of Configurations with Leading Edge Vortex Separation," AIAA Paper 76-417, San Diego, Calif., July 1976.

[8] Brune, G. W., Weber, J. A., Johnson, F. T., Lu, P., and Rubbert, P. E., "A Three-Dimensional Solution of Flows Over Wings with Leading Edge Vortex Separation," Part I, Engineering Document, NASA CR-132709, Sept. 1975.

[9] Wentz, W. H. and Kohlman, D. L., "Wind Tunnel Investigations of Vortex Breakdown on Slender Sharp-Edged Wings," NASA CR-98737, Nov. 1968.

[10] Earnshaw, P. B. and Lawford, J. A., "Low-Speed Wind-Tunnel Experiments on a Series of Sharp-Edged Delta Wings," Part 1, Royal Aircraft Establishment, RAE Tech. Note No. Aero. 2780, 1961.

[11] Elle, B. J., "An Investigation at Low Speed of the Flow Near the Apex of Thin Delta Wings with Sharp Leading Edges," Aeronautical Research Council, R&M No. 3282, April 1961.

[12] Lawford, J. A. and Beauchamp, A. R., "Low-Speed Wind-Tunnel Measurements on a Thin Sharp-Edged Delta Wing with 70° Leading-Edge Sweep, with Particular Reference to the Position of Leading-Edge-Vortex Breakdown," Aeronautical Research Council, R&M No. 3338, Nov. 1961.

[13] Earnshaw, P. B., "Measurements of Vortex-Breakdown Position at Low Speed on a Series of Sharp-Edged Symmetrical Models," Royal Aircraft Establishment, RAE TR No. 64047, Nov. 1964.

Lightning-Hazard Assessment: A First-Pass Probabalistic Model

Lee McKague*
General Dynamics, Fort Worth, Texas

Introduction

SOME kind of model is required to predict lightning-strike frequency and severity for a new aircraft system. No real model has existed for making such predictions. There also has been no model to help interpret data on lightning strikes to past or existing aircraft systems. Even so, such data has been collected for many years.

Historical evidence, therefore, exists to show the frequency with which aircraft are struck by lightning during flight. This frequency varies widely for various aircraft and service locations. Strike rates have been observed to range from about 2000 hours of service per strike for certain commercial carriers[1] to more than 200,000 hours of service per strike for T-33 jet trainers.[2] Damage records show the fleet distribution of these strikes to the various parts of a given airplane. These records, together with records of ground-based and airborne lightning-strike monitoring stations, provide insight to the severity of strikes.

All of this historical evidence is just that, historical. Predictive application of this evidence to planned aircraft systems relies at present on relatively gross judgments as to whether the new aircraft and mission are like a familiar past or present system.

Therefore, the purpose of this article is to describe a new and fundamental model with which aircraft lightning hazards can be analyzed and predicted. Use of the model for determining lightning-strike frequency of specific aircraft is discussed, and a framework is suggested for extending the use of the model. The model can be used by system planners to study service conditions, strategies, and alternatives that would reduce lightning hazards. It may also be used as a guide to design requirements and as an aid to prediction of service life costs for repair of lightning-strike damage.

Strike Frequency Model

This model considers three basic factors to be involved in calculating the lightning-strike frequency S of an airplane.

Received May 6, 1977.
Index cateories: General Aviation; Military Missions.
*Engineering Specialist, Fort Worth Division.